Dendrimer-based nanoparticles for cancer therapy

James R. Baker Jr.[1]

[1]*Division of Allergy and Clinical Immunology, Michigan Nanotechnology Institute for Medicine and Biological Sciences, Ann Arbor, MI*

Recent work has suggested that nanoparticles in the form of dendrimers may be a keystone in the future of therapeutics. The field of oncology could soon be revolutionized by novel strategies for diagnosis and therapy employing dendrimer-based nanotherapeutics. Several aspects of cancer therapy would be involved. Diagnosis using imaging techniques such as MRI will be improved by the incorporation of dendrimers as advanced contrast agents. This might involve novel contrast agents targeted specifically to cancer cells. Dendrimers can also be being applied to a variety of cancer therapies to improve their safety and efficacy. A strategy, somewhat akin to the "Trojan horse," involves targeting anti-metabolite drugs via vitamins or hormones that tumors need for growth. Further applications of dendrimers in photodynamic therapy, boron neutron capture therapy, and gene therapy for cancer are being examined. This presentation will cover the fundamentals of research utilizing dendrimers for cancer diagnosis and therapy. An evaluation of this new technologies will detail what advantage dendrimer based therapeutics might have over conventional cancer drugs.

Nanotechnology has led to a remarkable convergence of disparate fields including biology, applied physics, optics, computational analysis, and modeling, as well as materials science. Because of this, the application of nanoscale analytical, computational, and synthetic approaches to understanding and manipulating complex biological systems offers incredible potential for advances in the diagnosis and treatment of cancer.

Utilizing these advances, our interdisciplinary team at the University of Michigan Nanotechnology Institute for Medicine and Biological Sciences (M-NIMBS) has developed a number of technical solutions that provide a scaffold strategy so that multifunctional combinatory therapeutics can be designed and built. The scaffold is a dendritic polymer that is uniquely suited to biomedical applications in that it is a synthetic material that can be uniformly produced and yet has a diameter of only 5 nm. We have completed preliminary work providing proof of concept[1,2] and our team is now developing several nanodevices that have shown success in animal trials. These designed, multifunctional devices will have applications as targeted imaging and diagnostic agents for cancer at the earliest stages as well as multifunctional devices that can deliver therapeutics directly to cancer cells.

The technology we have developed will facilitate the concept of targeted, non-intrusive sensing, signaling, and intervention for cancer. If this polymer-based approach is successful *in vivo*, the targeting, sensing, and therapeutic conjugates can be interchanged to address varied tumor types or different genetic or enzymatic alterations associated with different cancers. Thus, this approach would yield common, interchangeable therapeutic platforms that transcend any single tumor or cellular abnormality.

Nanoparticle Cancer Therapeutics

Most cancer therapeutics are small drug molecules that after being ingested or injected into the bloodstream can easily diffuse through vascular pores and the extracellular matrix to reach tumors. Complex therapeutics that involve drug delivery mechanisms or imaging moieties have tended to be much larger. While the exact size of molecules that can easily transverse vascular pores from the bloodstream and reach tumor tissue is unclear, it is probably limited to the size of proteins (< 20 nm). Studies have documented that molecules 100 nm in diameter do not effectively diffuse across the vascular endothelium,[3] and even molecules 40 nm in diameter are problematic unless the endothelium is traumatized by radiation or heating.[4] The vasculature in early neoplastic lesions may be more restrictive.[5] Thus, designed nanoparticle-based therapeutics require a complex, multi-functional device that is still small enough to exit the vasculature in order to intimately interact with, and specifically eliminate cancer cells.

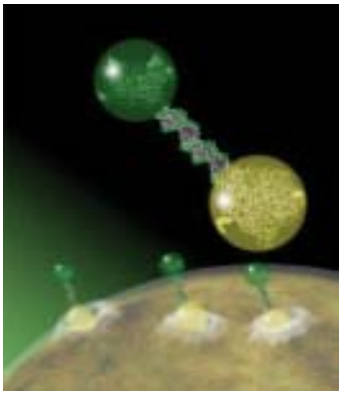

Figure 1. A binary nanoparticle targeting a cancer cell.

The nanoparticle therapeutic most often envisioned is a complex macromolecule that can identify specific targets on cancer cells *in vivo*. This device, however, will require more than the identification of specific pathophysiologic changes in particular cells. The analysis of cancer signature(s) must be coupled to one or more therapeutic agents that can be efficiently delivered to specifically kill the abnormal cells without collateral damage. This is difficult to accomplish since most chemotherapeutic agents will stop cell growth or induce apoptosis if inadvertently activated in normal cells.[6,7] Tumors often require higher doses of therapeutics since they have developed mechanisms of evading anticancer drugs, such as molecular pumps. Therapeutic agents will probably require several different mechanisms of action, working in parallel to prevent the development of resistant neoplasms. Finally, it will be important for the therapeutic agent to also monitor the response to therapy by identifying residual disease immediately after treatment. This is crucial since a few remaining cells may result in re-growth or worse, lead to a tumor that is resistant to therapy. Identifying residual disease at the end of therapy (rather than after tumor re-growth) will facilitate eradication of the few remaining tumor cells. Thus, an ideal therapeutic must have the ability to target cancer cells, image the extent of the tumor and sense its signatures, deliver a therapeutic, and monitor cells for their response. This is the goal for our nanotherapeutic.

Dendrimer-based Nanoparticles for Cancer Treatment

Two technical advances underlie our research. The first is the successful development of multifunctional nanodevices based on the dendritic polymer or dendrimer.[8] The second is the development of a linking strategy that allows the dendrimer molecules to be linked via complementary oligonucleotides.[1,2] In this review, we will discuss these two advances in sequence.

Prior Work on Dendrimers by Other Groups

The first technical result that underlies our proposal is the use of dendrimer. These polymers are synthesized as well-defined spherical structures ranging from 1 to 10 nanometers in diameter. Molecular weight and the number of terminal groups increase exponentially as a function of generation (the number of layers) of the polymer (**Figure 2**). Different types of dendrimers can be synthesized based on the core structure that initiates the polymerization process.[9] Poly(amidoamine) spherical dendrimers (PAMAM) with ethylene-diamine (EDA) as a tetravalent initiator core are used in our studies. These dendritic macromolecules are available commercially in kilogram quantities. We have now produced 100-gram lots of this material under current good manufacturing processes (GMP) for biotechnology applications. Dendrimers are characterized by electrospray-ionization mass spectroscopy (ES-MS), ^{13}C nuclear magnetic resonance spectroscopy (NMR), high-performance liquid chromatography (HPLC), size exclusion chromatography (SEC) with multi-angle laser light scattering, capillary electrophoresis (CE), and gel permeation chromatography (GPC) and a variety of gel electrophoresis techniques. These tests assure the uniformity of the polymer population and are essential to monitor quality control of dendrimer manufacture for GMP applications and *in vivo* usage. Importantly, extensive work has been completed with PAMAM dendrimers and *in vivo* studies have shown no evidence of toxicity when administered intravenously.[10,11]

Before we initiated our research, the performance of individual dendrimers had been demonstrated for essentially every desired component required for a viable anticancer nanostructure. PAMAM dendrimers have been used as a scaffold for the attachment of several types of biologic materials. This work has focused on the preparation of

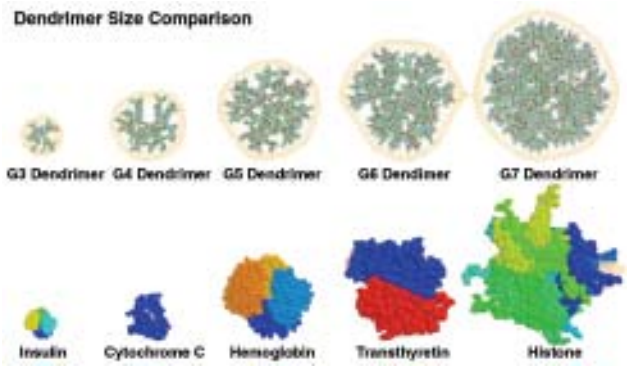

Figure 2. Several generations of spherical, dendritic polymers. Each generation increases the size, molecular weight and number of primary amine groups on the surface of the polymer.

dendrimer-antibody conjugates for use in *in vitro* diagnostic applications,[12] for the production of dendrimer-chelant-antibody constructs, and for the development of boronated dendrimer-antibody conjugates (for neutron capture therapy); each of these latter compounds is used as a cancer therapeutic.[13-16] Some of these conjugates have also been employed in the magnetic resonance imaging of tumors.[15,16] Results from these studies have documented that, when administered *in vivo*, antibodies can direct dendrimer-associated therapeutic agents to antigen-bearing tumors. Dendrimers also have been reported to enter tumors and carry either chemotherapeutic agents or genetic therapeutics. In particular, current studies show that cisplatin encapsulated in dendrimer polymers has increased efficacy and is less toxic.[17] Dendrimers have also been conjugated to fluorochromes and shown to enter cells. They can then be detected within the cell in a manner compatible with sensing apparatus for evaluation of physiologic changes within cells.[18] Finally, dendrimers have been constructed as differentiated block co-polymers where the outer portions of the molecule may be digested with either enzyme or light-induced catalysis.[19] This would allow the controlled degradation of the polymer to release therapeutics at the disease site and could provide a mechanism for an external trigger to release the therapeutic agents.

Multifunctional Single Dendrimer Nanodevices: *In Vitro* Testing

Over the past several years, we have made great progress in developing nanomolecular, multifunctional devices. We have produced a single device that has the different functions necessary for a targeted, active sensing, imaging therapeutic agent on a single dendritic molecule (**Figure 3**). This involves coupling of functional groups such as sensing units, MRI contrast agents, triggering devices, and targeting molecules to the surface of a generation 5 dendritic polymer (MW 25,000 daltons, diameter 5 nm). This has proven to be an arduous synthetic endeavor given the multiple conjugation steps that are required. Several challenging protect-deprotect steps are needed to produce such a multifunctional agent. This dendrimer-based agent has multiple functions and can be used as a testing platform to evaluate nanostructure and function. Because of prior reports where folic acid was coupled to proteins or drugs as a means of targeting cells (through the high affinity folate receptor), we adopted folate as an initial targeting ligand to attach to the dendrimer. In addition, because we had experience with coupling FITC to proteins, we used FITC as a signaling device to follow the fate of the dendrimer complex within cells. The techniques for this are described extensively by Quintana et al.[20] While this was not an optimized system as the FITC bleaches and the material could only be analyzed once, it provided a direct means to evaluate structural aspects of the polymer scaffold, cell delivery, and cell internalization.

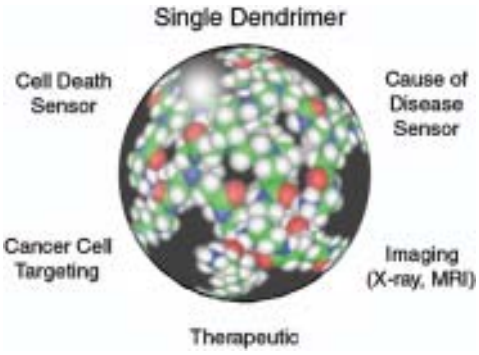

Figure 3. A single dendrimer can be used to produce a nanostructure by direct conjugation of multiple moieties directly to different branches of the molecule.

Research had suggested that when coupling folic acid to proteins or polymers, a net overall negative charge (predominantly carboxyl moieties) on the molecule surface was important for cellular targeting. However, PAMAM dendrimers are synthesized with a surface of primary amines, so we attempted to simply conjugate folate and FITC to amino surface dendrimers as a means to initiate our studies. When we placed this material *in vitro* with KB cells, which have elevated levels of the high affinity folate receptor, we saw very poor uptake that required several hours. More disconcerting, there was non-specific uptake in cell lines that lacked the high affinity folate receptor.

To improve this performance, we could have attempted many manipulations of the polymer surface or structure, all of which would have been synthetically complex and would have required considerable time to accomplish. Instead, we used computer modeling to evaluate several proposed polymer modifications that would improve delivery (**Figure 4**). Because differences in polymer surface charge were thought to be of paramount importance in the biological function of this scaffold, we first examined changes in the terminal groups on the polymer. Three different surface modifications were evaluated: carboxyl, hydroxyl and acetamide substitutions (**Figure 4**). The carboxyl modification previously reported to achieve efficient delivery to cells did appear to improve accessibility of folic acid molecules conjugated to the surface of the polymer. However, modeling studies also suggested that at higher concentrations of nanostructure, the carboxyl surface molecules would interact with secondary and tertiary amines in the dendrimer and would cause aggregation of these molecules. In contrast, both acetamide and hydroxyl surface modifications resulted in more compact structures in the dendrimer scaffold due to the loss of repulsion from

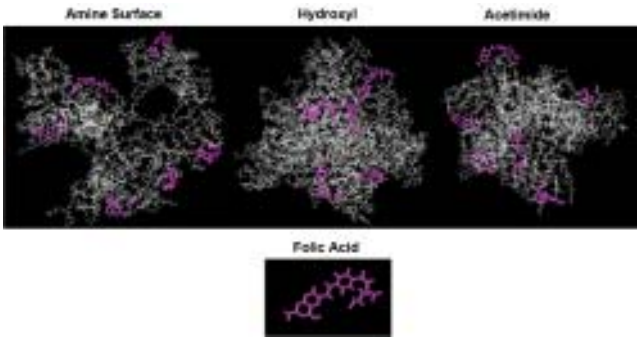

Figure 4. Modeling of folate-conjugated dendrimer nanostructure. Folate is exposed on the surface of the amine-surfaced polymer (left panel), but non-specific interactions between surface amines and cell dendrimers (middle panel) lacked non-specific interactions; however, the acetimide was predicted to have the folate in a surface position that was likely to interact with receptors on cells. This was proven to be correct in studies with intact cells expressing the receptor.

adjacent surface charged molecules (**Figure 4**). In addition, it appeared that all of the folic acids on the surface of the molecule were accessible for binding with cellular receptors in the acetamide molecule, while approximately two thirds of the targeting moieties in the hydroxyl molecule were available for binding. The modeling of the amine surface molecule (data not shown; see Quintana et al[20]) suggested that none of the folic acid molecules were externalized where they could bind to cellular receptors. This provided confidence that folic acid coupled polymer with neutralizing surface modifications might be able to efficiently target cells through the high affinity folate receptor.

Polymers with the three modified surfaces were synthesized and substituted with identical numbers of folic acid and FITC moieties. The activity of these molecules in targeting the folate receptor on KB cells *in vitro* was then evaluated and compared to that predicted in the molecular modeling. The results were dramatic (**Figure 5**). The cellular uptake of the acetamide and hydroxyl surface polymers was very rapid and very efficient. It occurred within minutes, peaking at approximately 20 or 30 minutes and appeared to resume after another 30 minutes, which corresponds to folate receptor recycling. Uptake was faster for the acetamide surface rather than the hydroxyl surface, confirming the modeling prediction that there were more surface folate groups available for binding. Also in accordance with the modeling, the carboxyl surface molecules initially had rapid uptake, but as the concentration of the nanostructure was increased, the uptake appeared to stop. This suggested that the molecules were aggregating and no longer available for binding to the cell surface receptor. The acetamide surface polymer continued to accumulate within the cells over time and appeared by confocal microscopy to internalize after approximately 4 to 6 hours.[20]

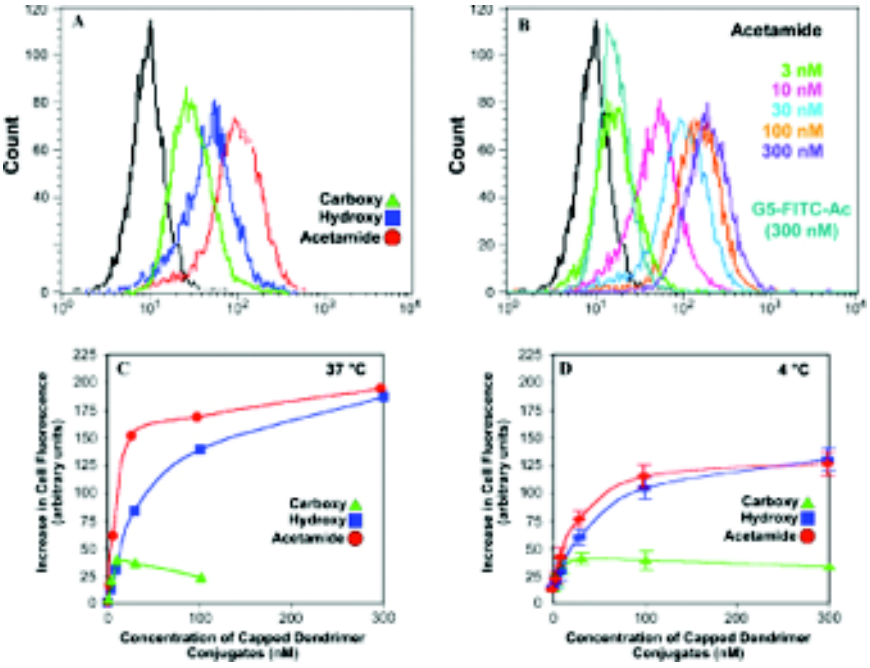

Figure 5. Binding of fluorescent dendrimer-folate conjugates to KB cells after 30 min incubation.
All panels except Panel D demonstrate experiments performed at 37 °C. Panel A demonstrates increases of cell-associated fluorescence after incubation with 30 nm of acetamide, hydroxyl, or carboxyl-surfaced dendrimer-folate conjugates. Panel B documents progressive increases of cell fluorescence after incubation with increasing concentrations of acetamide-surfaced fluorescent dendrimer-folate conjugate. Significant background fluorescence was not observed until the concentration of non-targeted complex reached 300 nm. Cell-associated fluorescence as a function of dendrimer-folate conjugate concentration is presented for each of the three types of dendrimer, at 37 °C in Panel C and at 4 °C in Panel D. Amine surfaced dendrimer-folate conjugates demonstrated no binding.
Reprinted with permission from Quintana et al.[20]

The next step was to develop a more complex device in which fluorescein, folate and drug were conjugated on a single polymer. This was accomplished by first acetylating approximately 80% of the primary amines on the surface of the polymer followed by the sequential attachment of folate, fluorescein, and one of two different drugs—either Taxol

or methotrexate (MTX). The drugs were attached through two linker mechanisms; one an ester linkage the other an amide linkage. The ester linkage should hydrolyze once the device internalized within the KB cell, while the amide linkage should retain drug and serve as a control. These conjugates were produced and tested in the KB cells. As shown in **Figure 6**, the polymers with the drug were internalized as efficiently as polymers that had only fluorescein on their surface. In addition, this targeted material was tested for the ability to induce cytotoxicity in the KB cells, by both an assay of mitochondrial activity (in a MTT assay) and by clonagenic assay. The ester-linked drug delivered with the folate was active as a cytotoxic agent, whereas the amide-linked drug was not. This suggested that the ester-linked drug was active, because the drug was released approximately 4 to 6 hours after internalization within the cell. The concentration of dendrimer-delivered MTX that induced cytotoxicity was compared to free methotroxate. In this culture system, the folate-targeted material was 5-to 10-fold more active than equipotent ?? free drug. We believe that this might be due to polyvalent receptor interactions and that the data suggest that targeting this drug to resistant cancer cells might be more effective than using free drug. In addition, 50% of bound nanostructure remained after acidic wash at 0 °C, while free folate is easily removed by this treatment. This suggested that the folate-dendrimer conjugates have increased binding stability on the cell surface, possibly through multiple receptor-folate interactions.

Multifunctional Single Dendrimer Nanodevices: *In Vivo* Testing

With the completion of the *in vitro* studies, we initiated animals trials to examine distribution and efficacy of the targeted nanotherapeutic. Data in this sub-section document tumor cell-targeted delivery and therapeutic effect of drug-dendrimer conjugates *in vivo.*

Biodistribution of Tritiated Dendrimers

We first examined the biodistribution and elimination of tritiated G5-^{3}H-FA to test its ability to target the FR-positive human KB tumor xenografts established in immunodeficient nude mice. The mice were maintained on a folate-deficient diet for the duration of the experiment to minimize the circulating levels of FA.[21] The free FA level achieved in the serum of the mice prior to the experiment approximated human serum levels.[22,23] Four pairs of nanoparticles were synthesized, with both members of each pair containing the same tracer. One member of each pair contained FA—one pair with, one pair without the antineoplastic drug MTX—while the other conjugate lacked FA and served as a non-targeted control with or without the drug.

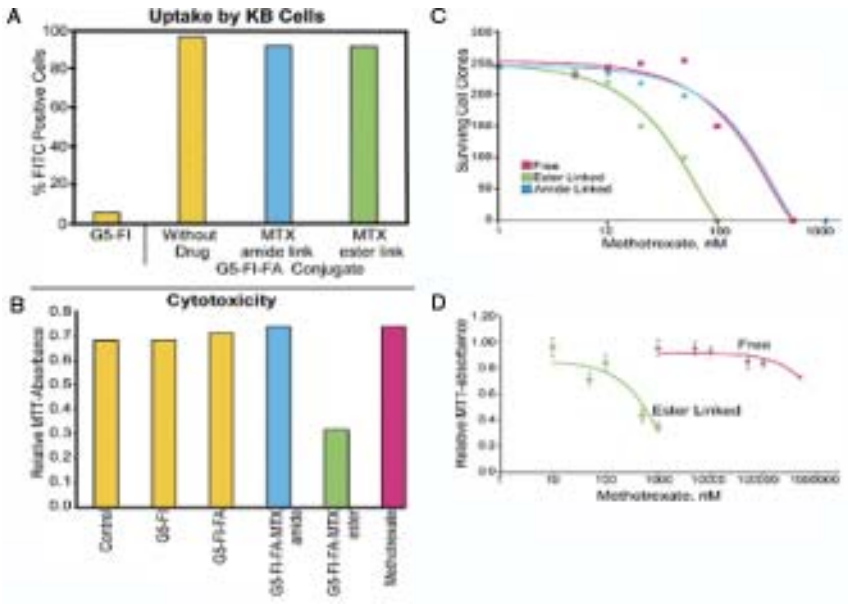

Figure 6. Studies examining intracellular delivery of methotrexate with a folate/FITC nanostructure. Panel A shows that the devices are readily taken into KB cells regardless of drug conjugate. Panel B shows that at 1000 uM only the conjugate where methotrexate is linked by an ester is acutely cytotoxic to the tumor cells. Panels C and D compare the efficiency in killing tumor cells and the acute cytotoxicity (respectively) of ester-conjugated drug and free methotrexate. The polymer delivered drug is 5 to 10 times more efficient at killing the KB cells. Reprinted with permission from Quintana et al.[20]

Mice were evaluated at various time points (5 minutes to 7 days) following intra-venous administration of the conjugates. Two groups of mice received either control non-targeted tritiated G5-^{3}H dendrimer or targeted tritiated G5-^{3}H-FA conjugate (**Figures 7A, 7B**). Full details of the study can be found in Kukowska-Latallo et al.[8] To summarize, the cumulative clearance of the targeted G5-^{3}H-FA over the first 4 days was lower than that of G5-^{3}H, which may reflect retention of G5-^{3}H-FA within tissues expressing folate receptors. While the kidney is the major clearance organ for these dendrimers, it is also known to express high levels of the FR on its tubules. The level of non-targeted G5-^{3}H in the kidney decreased rapidly and was maintained at a moderate level over the next several days (**Figure 7A**). In contrast, the level of G5-^{3}H-FA increased slightly over the first 24 hours,

most likely due to FR present on the kidney tubules. This was followed by a decrease over the next several days as the compound was cleared by the kidney (**Figure 7B**).

Biodistribution of Fluorescent Dendrimer Conjugate

To further confirm and localize the dendrimer nanoparticles within tumor tissue, dendrimers conjugated with 6-TAMRA (6T) were employed. Confocal microscopy images were obtained of tumor samples at 15 hours following intravenous injection of the targeted G5-6T-FA and the non-targeted G5-6T conjugates (**Figure 8**). The tumor tissue demonstrated a significant number of fluorescent cells with targeted-dye-conjugated dendrimer G5-6T-FA (**Figure 8C**) compared with those with non-targeted dendrimer (**Figure 8B**). Flow cytometry analysis of a single-cell suspension isolated from the same tumors showed higher mean channel fluorescence for tumor cells from mice receiving G5-6T-FA.

Cellular Internalization of Dendrimer Conjugate

Confocal microscopy also demonstrated that the conjugate is present in the tumors, attached to and internalized by many of the tumor cells. As the plane of view is moved from the top to the bottom of the tissue slide, cells are seen at their apical, medial, and finally their basal section. A given image typically appears in approximately 40 optical sections, and each section overlaps the optical section above and below it by 25% of its thickness. The medial sections of tumor cells show fluorescence throughout the cytosol from the 6-T of the conjugate, with the cell and nucleus boundary clearly visible (data not shown).

Targeted Drug Delivery to Tumor Cells Through the Folate Receptor

The efficacy of different doses of conjugates was tested on SCID C.B-17 mice bearing subcutaneous human KB xenografts and was compared with equivalent and higher doses of free MTX. Six groups of immunodeficient SCID mice with 5 mice in each group were injected subcutaneously on one flank with 5×10^6 KB cells in 200 µL PBS suspension. Twice a week, starting on day 4 after tumor implantation, the animals received via the tail vein an injection of either a conjugate containing MTX, a conjugate without MTX, free MTX, or saline as a control. The compounds were delivered in a 200 µL volume of saline per 20 g of mouse. The highest total dose of G5-FI-FA-MTX therapeutic used equals 55.0 mg/kg and is equivalent to a 5.0 mg/kg total cumulative dose of free MTX (**Figure 9**). The therapeutic dose was compared with three different (cumulative) doses of free MTX equivalent to 33.3 mg/kg, 21.7 mg/kg, and 5.0 mg/kg accumulated in 10 to 15 injections, based on mouse survival. Saline and the conjugate without MTX (G5-FI-FA) were used as controls. The body weights of the mice were monitored throughout the experiment as an

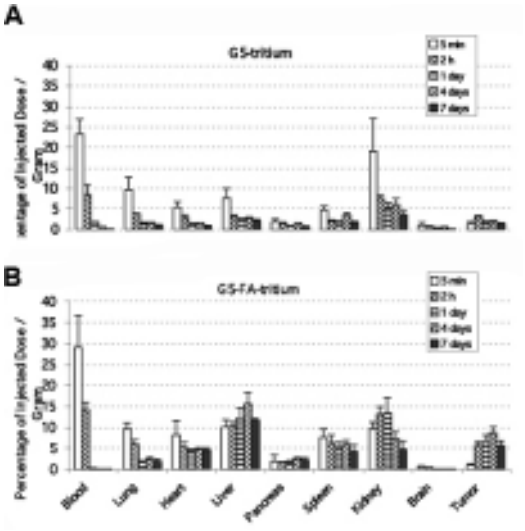

Figure 7. Biodistribution of radio-labeled non-targeted (A) and targeted (B) conjugate in nu/nu mice bearing KB xenograft tumor depicted as percentage of injected dose of dendrimer recovered per gram of organ (% ID/g ± SD). The values for different organs at 5 min, 2 h, and at 1, 4, and 7 days after delivery are the means ± SD of 3 to 5 mice.

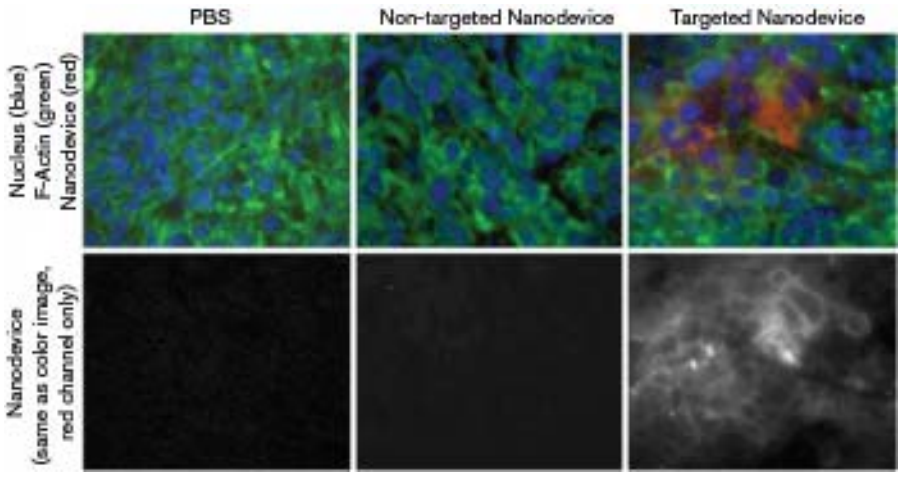

Figure 8. Fluorescence images of mouse KB cell tumor, harvested 15 hours after injection. There is greatly enhanced uptake of the folic acid targeted material by the tumor.

indication of adverse effects of the drug, and the changes of body weight demonstrated acute and chronic toxicity in the highest and in the second highest cumulative doses of free MTX equal to 33.3 mg/kg and 21.7 mg/kg, respectively (data not shown).

Although the two doses of free drug were affecting tumor growth, both became lethal by days 32 to 36 of the trial (**Figure 9**). The remaining experimental groups had very uniform body weight fluctuations non-indicative of toxicity when compared with control groups with saline or conjugate without MTX (data not shown). For the highest cumulative doses of free MTX used, histopathology analysis of the liver revealed advanced liver lesions, collections of inflammatory cells, and peri-portal inflammation. In contrast, neither the total accumulated dose of therapeutic conjugate equivalent to 5.0 mg/kg of free MTX nor free MTX at the same dose were toxic (**Figure 9**, O). Importantly, the therapeutic dose of conjugate that was equal to the lowest dose of free MTX used was as equally effective as the second highest dose of free MTX (21.7 mg/kg in 13 injections), whereas the free drug at this concentration had no effect on tumor growth (**Figure 9**, ▲). The conjugate without MTX also had no therapeutic effect when compared with injections of saline (**Figure 9**, △).

During a second 99-day trial, there was a statistically significant ($P < .05$) slower growth of tumors that were treated with G5-FI-FA-MTX or G5-FA-MTX conjugate without FITC, compared with those treated with free MTX, saline or non-targeted G5-FI-MTX conjugate. The equivalent dose of MTX delivered with both targeted conjugates to the surviving mice was higher than the dose of free MTX because all of the mice receiving free MTX had died by day 66 of the trial. The survival of mice from groups receiving G5-FI-FA-MTX or G5-FA-MTX conjugate indicates that tumor growth based on the end-point volume of 4 cm^3 can be delayed by at least 30 days. This value indicates the anti-tumor effectiveness of the conjugate because it mimics clinical end-points and requires observation of the mice throughout the progression of the disease. We have achieved a complete cure in one mouse treated with G5-FA-MTX conjugate at day 39 of the trial. The tumor in this mouse was not palpable for the next 20 days up to day 60 of the trial. At the termination of the trial,

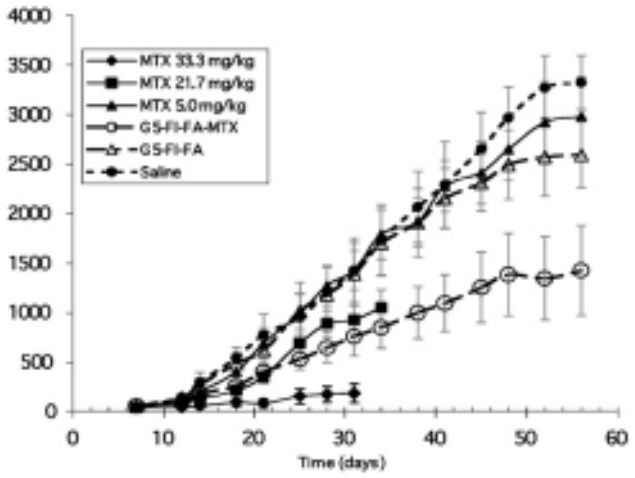

Figure 9. Tumor volume (mm^3) versus time of various treatment regiments. Total MTX dose of the polymer-delivered drug (open circles) was equal to the 21.7 mg/kg dose of free drug.

there were 3 (out of 8) survivors receiving G5-FA-MTX and 2 (out of 8) survivors receiving G5-FI-Fa-MTX. There were no mice surviving in the group receiving free MTX or in any other control group. **Figure 10** shows the mice dosed with MXT and those with MTX conjugated to targeted dendrimer. The effective dose of conjugate was not toxic based on weight change and histopathology examination.

Toxicity of Dendrimer Conjugates

All mice were observed for the duration of these studies for signs of dehydration, inability to eat or drink, weakness, or change in activity level. No gross toxicity, either acutely or chronically up to 99 days was observed regardless of whether or not the dendrimer conjugate contained MTX.

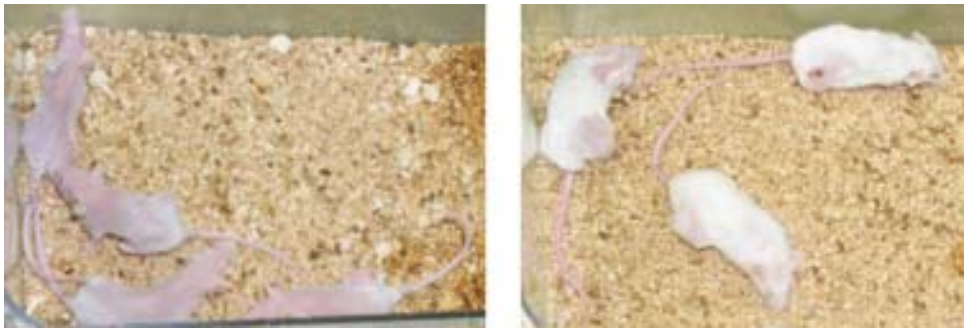

Figure 10. Mice on left dosed with methotrexate lose weight, hair and appear sick. Mice on right dosed with dendrimer-transported folate-targeted methotrexate exhibit no adverse effects from the chemotherapy. Drug-induced necrosis of the tumor on the flank of the mouse in the upper right corner.

Prior Work on Complementary Oligonucleotide Linkages by M-NIMBS

The second enabling technology, which we developed over the past few years, is clustering dendrimers with different functions using complementary oligonucleotides that are attached to each dendrimer (**Figure 11**). This approach allows greater flexibility than using a single dendrimer with multiple functions, as the clusters are self-assembling without additional chemical alterations that could harm the units. We expect the oligos to be susceptible to nuclease digestion, which would allow the breakdown of the device after it is delivered to the cells. Since the largest subunit will be a G5 (25 kDa), the fragments would be eliminated through the kidney. Finally, using different sets of complementary oligonucleotides, the ratios of different subunits in the cluster could be controlled allowing for construction of combinatorial libraries of dendrimer-linked anticancer therapeutics, imaging and targeting agents.

Development of a multifunctional nanostructure that does not require all of the synthetic chemistry involved to be performed on a single molecule is attractive for several reasons. Chemical modifications of a single polymer required for coupling different components can damage other components already on the device. Each specific device must be produced individually. While we clearly have been able to produce this type of agent (as described in the description above), an alternative approach uses a structure to assemble dendritic polymer components into a single molecule. This allows us to place each component of the nanostructure on a different polymer and assemble them as a single, supramolecular assembly. There are a number of possible architectures for such an assembly; a star topology is shown in **Figure 11**.

We initiated our studies with the simplest conjugation strategy: two dendrimers linked via complimenary oligonucleotides in a dumbell configuration (**Figure 12**). We wanted to test the ability of this novel dendrimer platform to target to cancer cells over-expressing folate receptor by conjugating a targeting (FA) and an imaging (FITC) molecule to two different dendrimers, which are then linked with complementary oligonucleotides (34 bp). The prototype DNA-assembled nanocluster of the FA-conjugated dendrimer and FITC-conjugated dendrimer would then be characterized and evaluated *in vitro* to test tumor cell–specific binding and internalization.

The entire synthesis of the cluster agent consists of three conjugation reactions and one hybridization reaction (**Scheme 1**). The acetylation reaction of the amine-terminated dendrimer is very efficient and stoichiometrically controllable as reported by Majoros et al.[24] To determine the sub-stoichiometric equivalent of acetic anhydride to the dendrimer, the number of the terminal primary amine groups on the dendrimers was first determined to be 110 (as compared to the theoretical value of 128) by potentiometric titration and SEC-MALLS measurement. This result is consistent with other findings explaining the inherent structural defects from incomplete reactions or other problems in the divergent synthesis of the dendrimer causing: missing repeating unit, intramolecular cyclization, dimer formation and retro-Michael reaction in dendrimers.[9,25,26] The addition of 82 molar equivalents of acetic anhydride to the terminal, primary amine groups of the dendrimer in the presence of a triethylamine base resulted in partial conversion of the primary amine groups to acetamide moieties. The degree of acetylation was measured by ^{1}H NMR, using the specific acetyl proton peak at 1.9 ppm. The increasing intensity of this signal indicated that an average of 80 acetyl groups were added to each dendrimer (G5-Ac_{80}-$(NH_2)_{30}$). The yield of this reaction was 85% by weight (782 mg) and the calculated molecular weight of the final product was 28,752 g/mol.

Figure 11. Schematic diagram of an oligonucleotide cluster agent. Oligonucleotides are covalently conjugated to generation 3 dendrimers with specific functional groups. Complementary oligonucleotides are coupled to a core generation 5 dendrimer. Different units are then combined in physiologic conditions and aggregate into a device. Oligonucleotides are designed to assure the specificity of the hybridization and the stability of the duplex at physiologic conditions.

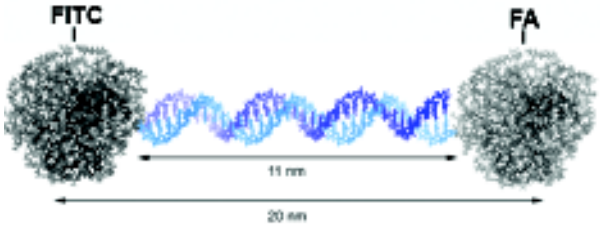

Figure 12. Prediction of overall dimension of the target DNA-linked functional dendrimer cluster agent by computer modeling (Insight II®). The DNA linker (34bp) is 11 nm and the center-to-center distance of the two functional dendrimers is estimated to be 20 nm. FITC and FA are schematically shown on the periphery of the dendrimer.

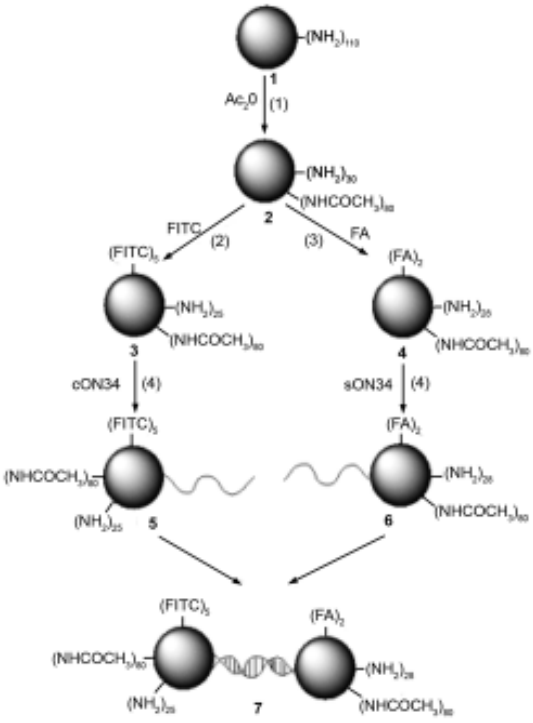

Scheme I. Synthetic scheme for the preparation of a DNA-linked cluster of G5-FITC and G5-FA dendrimers. (1) triethylamine, MeOH, 16h; (2) DMSO; (3) EDC in DMF:DMSO (3:1; v/v); (4) 0.1M EDC/0.1 M Imidazole (pH 6.0) in 0.5 M LiCl; (5) 10 mM phosphate buffer (pH 7.4), 150 mM NaCl, annealed at 90°C for 10 min, then cooled to room temperature over 3 h.

FITC was qualitatively documented to be conjugated to the dendrimer by TLC analysis, which showed that FITC conjugated to dendrimer was being retained at the origin, while non-conjugated free FITC migrated at the solvent front ($R_f = 0.72$). The approximate number of conjugated FITC molecules per G5 dendrimer was determined by UV and ^{1}H NMR spectroscopy. The A at 502 nm shows a linear relationship with the conjugate concentration; extinction coefficient = 246600 $M^{-1}cm^{-1}$. From the calibration curve of the free dye (data not shown), the average number of FITC molecules per dendrimer was calculated to be 5. This was consistent with ^{1}H NMR spectroscopy evaluation using the sum of the integrals of the aromatic protons of FITC.

The condensation reaction between the active ester of folic acid and the remaining primary amines on the partially acetylated dendrimer was conducted in the presence of water-soluble carbodiimide (1-ethy-3-(3-dimethylamino-propyl) carbodiimide; EDC). The UV spectrum of the conjugate in water at a concentration of 2 nM showed a maximum peak at 280 nm and a broad shoulder at 370 nm. From the calibration curve of the free FA, the number of FA molecules was calculated to be 2 ± 0.4, when five molar equivalents of FA to the dendrimer were used in the conjugation reaction. From the integral ratio of aromatic protons in FA molecules (8.6, 8.0, 7.6, 6.7 ppm) to the signal at 1.8 ppm, which corresponds to the methyl protons in the acetamide groups on the surface, the average number of FA moiety in the conjugate was calculated to be 2.5 molecules of FA residue per dendrimer, which agrees with the UV result. Synthetic DNA has been used as a tool to self-assemble nanoscale objects[27-29] and the attachment of DNA oligonucleotides to organic or inorganic polymers, such as proteins and metallic nanoparticles, has been studied extensively.[27-29] Recently, covalent attachment of oligonucleotide to either the core or the periphery of the dendron of various dendrimers has been reported, where SH-modified oligonucleotides or SH-core dendrons are coupled to a linker maleimide group or oligonucleotide to produce the conjugates.[30,31]

Figure 13 shows a representative example of AFM images of the DNA-linked dendrimer nanoclusters adsorbed to a mica substrate in dry state. Some of the larger objects appeared to be aggregates of many individual dendrimers and/or dendrimer clusters. However, there are a number of smaller, dumbbell-shaped clusters whose dimensions are consistent with the ones expected for individual DNA-linked dendrimers. Measuring the average volume (286 ± 80 nm^3) of the imaged objects suggests assemblies of two or three dendrimers, which is close to that expected in a dimeric dendrimer cluster. Note that the very low aspect ratio of these topographical features helps to minimize tip convolution effects in the volume measurement.[26] Some of the particles have larger volumes indicating that more than two dendrimers with a few oligonucleotides attached have assembled into a cluster. The distances between the linked particles are consistently approximately 20 nm, which is in good agreement with the theoretical length of the hybridized cON50-sON50 oligonucleotides as schematically shown in **Figure 13**.

We employed phosphoramidate chemistry developed by Chu et al[32] between the 5′ phosphate group of single-stranded DNA and the terminal amine group of the PAMAM dendrimer to covalently attach a synthetic oligonucleotide DNA to the dendrimer surface. Given the potential for interaction of the positively charged amine-terminated dendrimer and the negatively charged DNA, charge interaction must be prevented to avoid insoluble complex formation.[33] Thus, the partial capping of the surface primary amine groups with acetamide groups was also necessary to minimize electrostatic interactions at physiological pH. In

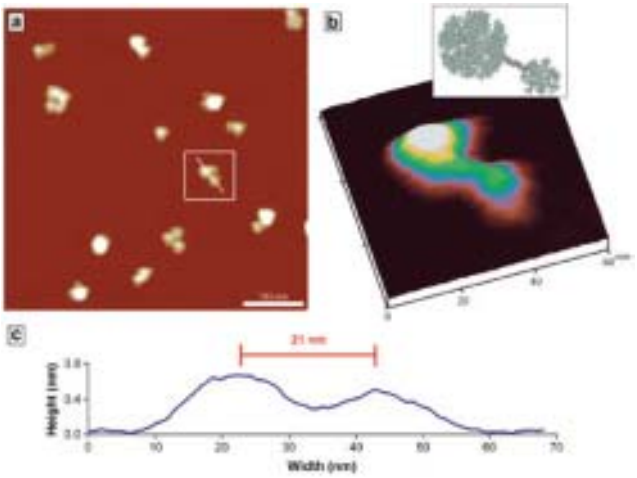

Figure 13. (a) A representative image of DNA-linked G7-G5 dendrimer nanocluster on mica (500 nm × 500 nm), (b) a three-dimensional image of one single dimeric cluster arrowed in (a), and (c) a line scan analysis of the cluster according to the white line in (a). The intra-dendrimer distance was theoretically calculated to be 20 nm and observed to be 21 ± 2 nm on average.

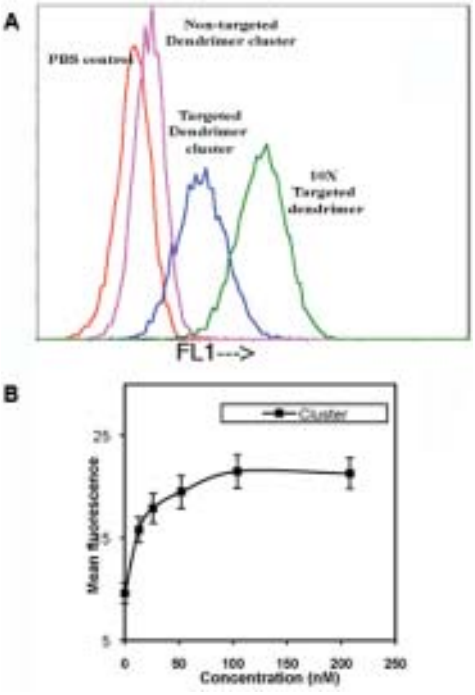

Figure 14. Binding of DNA-linked functional dendrimers to KB cells after 1 h incubation. (a) Gradual increase of cell-associated fluorescence after incubation with increasing concentrations of DNA-linked G5-FITC and G5-FA dendrimer cluster. (b) The concentration-dependent saturation curve indicates specific binding of the DNA-linked cluster to KB cells over-expressing folate receptor.

addition, the use of molar excesses of either dendrimer or DNA in conjunction with salt (LiCl) prevented complex formation. As we have reported earlier[1] and suggested by DeMattei et al,[34] minimizing non-specific interaction of DNA and dendrimer and limiting the number of DNA on each dendrimer are crucial to constructing dendrimer components into a nanostructure with defined size and shape.

In this study, we used a five molar excess of dendrimer to DNA so that the number of DNA conjugated to the dendrimer would be limited to approximately a single strand per dendrimer. In this way, any un-reacted dendrimer was removed after the hybridization reaction of the DNA-conjugates by centrifugal filtration using a 100 kDa MWCO membrane, which retains the desired DNA-linked functional dendrimer nanocluster. Since the cluster is assumed to have a dumbbell-like structure with a theoretical molecular weight of approximately 86 kDa, this separation method allows for separation of the target nanostructure from the unlinked globular FITC-conjugated or FA-conjugated dendrimers or unhybridized DNA-dendrimer components.

FA is known to be internalized into cells through a high affinity, receptor-mediated process.[35] The high affinity receptor for folic acid is over-expressed on a number of human tumors, including cancers of the ovary, kidney, uterus, testis, brain, colon, lung and myelocytic blood cells.[36-39] The KB cells we employed for this study are a human epidermoid carcinoma type cell that over-expresses folate receptors, especially when grown in low folic acid medium. Since the affinity of folate conjugates for the cell surface folate receptors is high (K_D~ 10^{-10}M), the folic acid modification of dendrimers allows the specific delivery of diagnostic and therapeutic agents to cancer cells. Thus, dendrimer folic acid conjugates linked to either a single drug molecule or assembly of molecules can bind to and enter receptor-expressing tumor cells via folate-mediated endocytosis.[20,40]

The binding of the cluster nanodevice to KB cells showed concentration-dependent uptake with saturation occurring at around 40 nM (**Figure 14A**). The sigmoidal profile of the dose-dependent curve suggests that the uptake of the dendrimer cluster is saturable, indicating the binding of the cluster to the KB cells over-expressing folate receptors with an apparent affinity of at least 15 nM to achieve 50% of maximal binding. The saturation of the binding curve occurred at 40 nM, which is comparable to the binding capacity (200 nM) of the single dendrimer nanodevices.[20] This binding capacity of the cluster allowed for a 200% increase in the mean fluorescence measured at 500 nm after incubation for 1 hour at 37°C with a concentration of 40 nM. In addition, increases in cell fluorescence from the

binding of the cluster nanodevice were effectively blocked by the addition of free FA in the medium.

The binding observed in the flow cytometry studies (**Figure 15**) was further confirmed in confocal microscopic images of the cells. A significant difference of fluorescence from the PBS control was not obtained due to the low concentration of the DNA-linked cluster agent (80 nM) as well as autofluorescence of the control cells in the measured emission wavelength (515 nm). However, the confocal analysis documented the presence of the cell-associated fluorescence of the DNA-linked dendrimer cluster both in the periphery of the cell membrane and at the cytoplasm of the cell, suggesting that the clusters had been internalized across the membrane into the cell.

We also used several control samples to show that the cell-associated FITC fluorescence originated from the DNA-linked FITC-dendrimer and FA-dendrimer cluster rather than a non-specific aggregate of the two functional

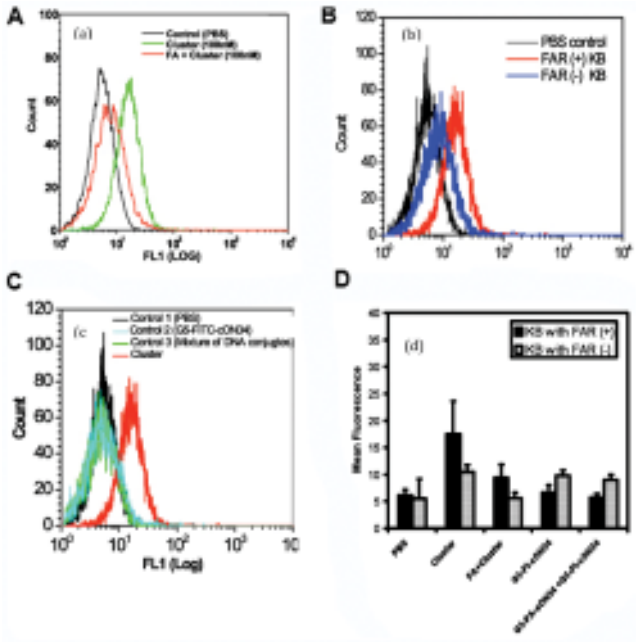

Figure 15. (a) Competitive inhibition of the cluster agent (40 nM) by free FA (5 mM). (b) The cluster failed to bind to the folate receptor down-regulated KB cells (FAR-) (c) Control groups (2: G5-FITC-cON34; 3: mixture of G5-FA-sON34 and G5-FITC-cON34 with no annealing process) showed no non-specific binding, suggesting a clustering of dendrimer-DNA conjugates did not occur *in vitro* without *in situ* DNA hybridization reaction. (d) Comparison of the mean fluorescence intensity of the cluster and the cluster antagonized by free FA, with controls (G5-FITC-cON34 and the mixture of the DNA-dendrimer conjugates.

dendrimers (without regard to the presence of a duplex DNA linkage). The mixture of the DNA-conjugated dendrimer, which did not undergo the annealing process, bound poorly to the KB cells. The DNA-conjugated G5-FITC dendrimer (G5-FITC-cON34) alone did not show significant binding, suggesting the non-specific binding of the G5-FITC-cON34 is not significant. These control experiments document that non-specific associations of the DNA-conjugated functional dendrimers with the cell surface is not the cause of the cell binding and uptake we observed.

Summary

In summary, nanoparticle therapeutics based on dendrimers and oligonucleotide linked dendrimers appear to be able to improve the therapeutic index of cytotoxic drugs by direct delivery of the drugs to cancer cells. There is also hope that delivering drug by this approach could overcome drug resistance in tumor cells via bypassing p-glycoprotein pumps that would normally export drugs that must diffuse into cells. Further toxicological studies and GMP synthesis of this material are underway to allow the initiation of clinical trials.

Disclosures

Conflict-of-interest disclosure: The author is a consultant and major equity holder in NanoBio, Avidimer Therapeutics, and JTM Research, LLC.
Off-label drug use: None disclosed.

Correspondence

James R. Baker, MD, Division of Allergy and Clinical Immunology, Michigan Nanotechnology Institute for Medicine and Biological Sciences, 9220 MSRB III, 1150 West Medical Center Drive, Ann Arbor, MI 48109–5648; Phone: 734-647-2777; Fax: 734-936-2990; e-mail: jbakerjr@umich.edu

References

1. Choi YS, Mecke A, Orr BG, Holl MMB, Baker JR. DNA-directed synthesis of generation 7 and 5 PAMAM dendrimer nanoclusters. Nano Lett. 2004;4:391-397.
2. Choi YS, Thomas T, Kotlyar A, Islam MT, Baker JR. Synthesis and functional evaluation of DNA-assembled polyamidoamine dendrimer clusters for cancer cell-specific targeting. Chem Biol. 2005;12:35-43.
3. Kong G, Braun RD, Dewhirst MW. Characterization of the effect of hyperthermia on nanoparticle extravasation from tumor vasculature. Cancer Res. 2001;61:3027-3032.
4. Kong G, Braun RD, Dewhirst MW. Hyperthermia enables tumor-specific nanoparticle delivery: effect of particle size. Hyperthermia enables tumor-specific nanoparticle delivery: effect of particle size. Cancer Res. 2000;60:4440-4445.
5. Bilbao R, Bustos M, Alzuguren P, et al. A blood-tumor

barrier limits gene transfer to experimental liver cancer: the effect of vasoactive compounds. Gene Therapy. 2000;7:1824.
6. Culver KW. Clinical applications of gene therapy for cancer. Clin Chem. 1994;40:510.
7. Rosenberg SA. The immunotherapy and gene therapy of cancer. J Clin Oncol. 1992;10:180.
8. Kukowska-Latallo J, Candido K, Cao ZY, et al. Nanoparticle targeting of anticancer drug improves therapeutic response in animal model of human epithelial cancer. Cancer Res. 2005;65:5317.
9. Tomalia DA, Naylor AM, Goddard WA. Starburst dendrimers: molecular-level control of size, shape, surface chemistry, topology, and flexibility from atoms to macroscopic matter. Angew Chem Int Ed Engl. 1990;29:138-175.
10. Bourne MW, Margerun L, Hylton N, et al. Evaluation of the effects of intravascular MR contrast media (gadolinium dendrimer) on 3D time of flight magnetic resonance angiography of the body. J Mag Res Imag. 1996;6:305.
11. Roberts JC, Bhalgat MK, Zera RT. Preliminary biological evaluation of polyamidoamine (PAMAM) Starburst™ dendrimers. J Biomedl Mat Res. 1996;30:53.
12. Singh P, Moll F III, Lin SH, et al. Starburst™ dendrimers: enhanced performance and flexibility for immunoassays. Clin Chem. 1994;40:1845.
13. Barth RF, Adams DM, Soloway AH, Alam F, Darby MV. Boronated starburst dendrimer-monoclonal antibody immunoconjugates: evaluation as a potential delivery system for neutron capture therapy. Bioconj Chem. 1994;5:58.
14. Barth RF, Soloway AH, Adams DM, Alam F. Delivery of boron-10 for neutron capture therapy by means of monoclonal antibody-Starburst dendrimer immunoconjugates. Plenum Press: New York; 1992.
15. Wu C, Brechbiel MW, Kozak RW, Gansow OA. Metal-chelate-dendrimer-antibody constructs for use in radioimmunotherapy and imaging. Bioorg Med Chem Lett. 1994, 4, 449.
16. Wiener EC, Magnin RL, Gansow OA, et al. Dendrimer-based metal chelates: a new class of magnetic resonance imaging contrast agents. Magn Reson Med. 1994;31:1.
17. Duncan R, Malik N. Control Rel. Bioact Mater. 1996;23:105.
18. Barker SL, Shortreed MR, Kopelman R. Utilization of lipophilic ionic additivies in liquid polymer film optodes for selective anion activity measurements. Anal Chem. 1997;69:990.
19. Urdea MS, Horn T. Dendrimer development. Science. 1993;261:534.
20. Quintana A, Raczka E, Piehler L, et al. Design and function of a dendrimer-based therapeutic nanodevice targeted to tumor cells through the folate receptor. Pharmaceutical Res. 2002;19:1310-1316.
21. Mathias CJ, Wang S, Waters DJ, Turek JJ, Low PS, Green MA. Indium-111-DTPA-folate as a potential folate-receptor-targeted radiopharmaceutical. J Nucl Med. 1998;39:1579-1585.
22. Nelson BC, Pfeiffer CM, Margolis SA, Nelson CP. Solid-phase extraction-electrospray ionization mass spectrometry for the quantification of folate in human plasma or serum. Anal Biochem. 2004;325:41-51.
23. Belz S, Nau H. Determination of folate patterns in mouse plasma, erythrocytes, and embryos by HPLC coupled with a microbiological assay. Anal Biochem. 1998;265:157-166.
24. Majoros IK, B, Woehler S, Bull T, Baker JR Jr. Acetylation of poly(amidoamine) dendrimers. Macromolecules. 2003;36:5526-5529.
25. Peterson J, Allikmaa V, Subbi J, Pehk T, Lopp M. Structural deviations in poly(amidoamine) dendrimers: a MALDI-TOF MS analysis. Eur Polymer J. 2003;39:33-42.
26. Kallos GJ, Tomalia DA, Hedstrand DM, Lewis S, Zhou J. Molecular weight determination of a polyamidoamine starburst polymer by electrospray ionization mass spectrometry. Rapid Comm Mass Spectrom. 1991;5:383-386.
27. Alivisatos P. The use of nanocrystals in biological detection. Nat Biotechnol. 2004; 22:47-52.
28. Nam JM, Thaxton CS, Mirkin CA. Nanoparticle-based bio-bar codes for the ultrasensitive detection of proteins. Science. 2003;301:1884-1886.
29. Elghanian R, Storhoff JJ, Mucic RC, Letsinger RL, Mirkin CA. Selective colorimetric detection of polynucleotides based on the distance-dependent optical properties of gold nanoparticles. Science. 1997;277:1078-1081.
30. Majoros IJ, Williams CR, Baker JR Jr. Current dendrimer application in cancer diagnosis and therapy. Curr Top Med Chem. 2008;8:1165-1179.
31. Bell SA, McLean ME, Oh SK, et al. Synthesis and characterization of covalently linked singe-stranded DNA oligonucleotide-dendrom conjugates. Bioconj Chem. 2003;14:488-493.
32. Chu BCF, Wahl GM, Orgel LE. Derivatization of unprotected polynucleotides. Nucleic Acids Res. 1983;11:6513-6529.
33. Uppuluri S, Swanson DR, Piehler LT, Li J, Hagnauer GL, Tomalia DA. Core-shell tecto(dendrimers): 1. Synthesis and characterization of saturated shell models. Adv Mater. 2000;12:796-800.
34. DeMattei CR, Huang BH, Tomalia DA. Nano Lett. 2004;4:771-777.
35. Leamon CP, Low PS. Delivery of macromolecules into living cells: a method that exploits folate receptor endocytosis. Proc Natl Acad Sci U S A. 1991;88:5572-5576.
36. Lu YJ, Low PS. Folate-mediated delivery of macromolecular anticancer therapeutic agents. Adv. Drug Delivery Rev. 2002;54:675-693.